TECHNICAL REPORT
NATICK/TR-15/012

AD _____

CENTRIFUGAL BLOWER FOR PERSONAL AIR VENTILATION SYSTEM (PAVS) PHASE I

by
Daniel P. Rini
and
Benjamin A. Saarloos

RINI Technologies, Inc.
Oviedo, FL 32765

February 2015

Final Report
May 2007 – November 2007

Approved for public release; distribution is unlimited

Prepared for
U.S. Army Natick Soldier Research, Development and Engineering Center
Natick, Massachusetts 01760-5019

DISCLAIMERS

The findings contained in this report are not to be construed as an official Department of the Army position unless so designated by other authorized documents.

Citation of trade names in this report does not constitute an official endorsement or approval of the use of such items.

DESTRUCTION NOTICE

For Classified Documents:

Follow the procedures in DoD 5200.22-M, Industrial Security Manual, Section II-19 or DoD 5200.1-R, Information Security Program Regulation, Chapter IX.

For Unclassified/Limited Distribution Documents:

Destroy by any method that prevents disclosure of contents or reconstruction of the document.

REPORT DOCUMENTATION PAGE

Form Approved
OMB No. 0704-0188

PLEASE DO NOT RETURN YOUR FORM TO THE ABOVE ADDRESS.

1. REPORT DATE *(DD-MM-YYYY)*	2. REPORT TYPE	3. DATES COVERED *(From - To)*
11-02-2015	Final	May 2007 – November 2007

4. TITLE AND SUBTITLE

CENTRIFUGAL BLOWER FOR PERSONAL AIR VENTILATION SYSTEM (PAVS) – PHASE I

5a. CONTRACT NUMBER
W911QY-07-C-0070

5b. GRANT NUMBER

5c. PROGRAM ELEMENT NUMBER

6. AUTHOR(S)

Daniel P. Rini and Benjamin A. Saarloos

5d. PROJECT NUMBER

5e. TASK NUMBER

5f. WORK UNIT NUMBER

7. PERFORMING ORGANIZATION NAME(S) AND ADDRESS(ES)

RINI Technologies, Inc.
582 S. Econ Circle
Oviedo, FL 32765

8. PERFORMING ORGANIZATION REPORT NUMBER

NATICK/TR-15/012

9. SPONSORING / MONITORING AGENCY NAME(S) AND ADDRESS(ES)

U.S. Army Natick Soldier Research, Development and Engineering Center
ATTN: RDNS-SEW-EMU (B. Laprise)
Kansas Street, Natick, MA 01760-5019

10. SPONSOR/MONITOR'S ACRONYM(S)
NSRDEC

11. SPONSOR/MONITOR'S REPORT NUMBER(S)

12. DISTRIBUTION / AVAILABILITY STATEMENT

Approved for public release; distribution is unlimited

13. SUPPLEMENTARY NOTES

SBIR data rights period expired November 23, 2012.

14. ABSTRACT

Report Developed under Small Business Innovation Research Contract. A Personal Air Ventilation System (PAVS) blower was designed beginning with an analytical design based on aerodynamic similarity. A radial-axial blower design was chosen to achieve the highest possible efficiency within the size constraints of the system. The blower is able to deliver 10 ft3/min of air at 5 in H2O (1243 Pa) pressure drop while consuming less than 15 W of electrical power. Computational fluid dynamics (CFD) iterations of the blower were used to minimize losses and increase efficiency through adjustments of the specific blower geometry. CFD outputs included the total and static pressure rise, as well as shaft power input. The shaft power requirement was matched with a commercial off-the-shelf (COTS) motor such that the electrical power input was under 15 W. The motor voltage and current were matched with standard military battery cells of various chemistries, yielding run-times that exceeded the 4-hr run time requirement. A full 3D system model was constructed, and the final system volume and weight (including battery) were less than the 60 in3 and 2 lb requirements. A stereolithograph mock-up of the blower was built and delivered to demonstrate functionality.

15. SUBJECT TERMS

COOLING	SBIR REPORTS	AXIAL FLOW FANS	OFF THE SHELF EQUIPMENT
BLOWERS	LIGHTWEIGHT	CENTRIFUGAL FORCE	HEAT STRESS (PHYSIOLOGY)
AIR FLOW	VENTILATION	PORTABLE EQUIPMENT	PERSONAL COOLING SYSTEMS
EFFICIENCY	EVAPORATION	INTEGRATED SYSTEMS	PROTOTYPES
COMPUTATIONAL FLUID DYNAMICS		PAVS (PERSONAL AIR VENTILATION SYSTEM)	

a. REPORT	b. ABSTRACT	c. THIS PAGE	17. LIMITATION OF ABSTRACT	18. NUMBER OF PAGES	19a. NAME OF RESPONSIBLE PERSON
U	U	U	SAR	24	Brad Laprise

19b. TELEPHONE NUMBER *(include area code)*
508-233-5440

This page intentionally left blank

TABLE OF CONTENTS

LIST OF FIGURES

LIST OF TABLES

CENTRIFUGAL BLOWER FOR THE PERSONAL AIR VENTILATION SYSTEM (PAVS) – PHASE I

1. INTRODUCTION

A Personal Air Ventilation System (PAVS) provides cooling to an individual by enhancing sweat evaporation. Even though the ambient air may be warm (i.e. > 35°C), provided the air is relatively dry, there is significant potential to remove heat as illustrated in Figure 1.

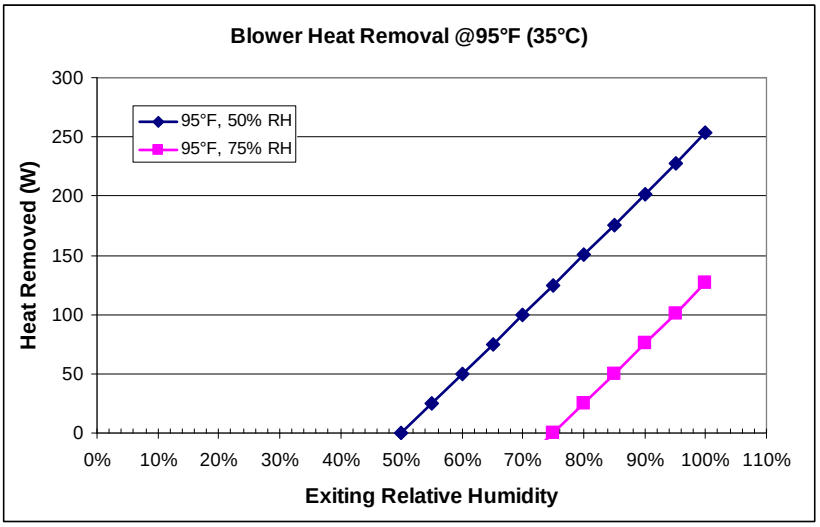

Figure 1: PAVS heat removal potential - 10 Cubic Feet per Minute (CFM), 95°F ambient air)

Since the PAVS system is extra equipment that the user will have to carry, the system must be compact and efficient to provide a true benefit to the user. The requirements of the PAVS in this development effort are summarized as follows:

- Air Flow: 10 CFM (0.28 m3/min) through (2) C2A1 filters (in parallel)
- Backpressure: 5 inH2O (1243 Pa)
- Power Consumption: 15 W max
- Weight & Volume
  - < 2 lb, < 60 in^3
  - Includes blower, motor, power source
  - Excludes filters
- Depth Dimension < 2 in
- Run-time: 4 hr

Given the 15 W maximum power consumption, a review of Commercial Off-The-Shelf (COTS) blowers reveals about a 2X factor difference between available performance and the performance required for the PAVS (see Figure 2). Thus, a significant efficiency improvement over COTS performance is required.

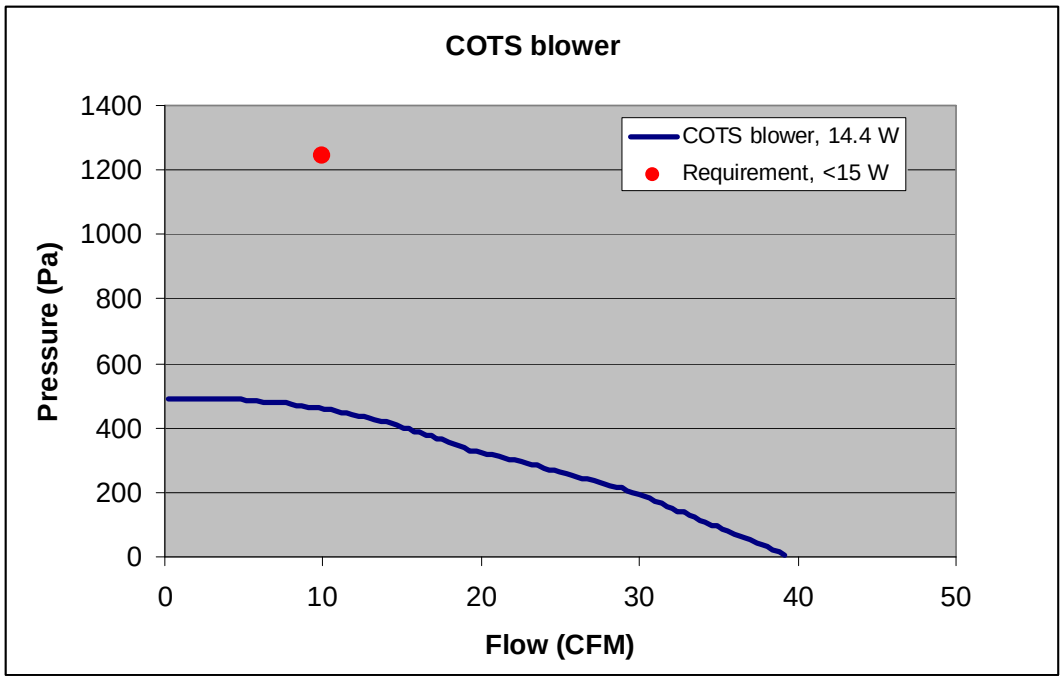

Figure 2: COTS blower performance vs. PAVS requirement

2. AXIAL-RADIAL BLOWER

A blower that meets the requirements of this development effort requires a high aerodynamic efficiency. The feasibility of this efficiency can be examined with n_s-d_s plots. N_s is the specific speed of the turbo-machine, and d_s the specific diameter (see definitions below). The plots are estimated maximum achievable efficiencies based on historical turbo-machinery data. It should be emphasized that they do NOT necessarily provide a precise efficiency for a given turbo-machine, but they do give a "ball-park" estimate of what efficiencies are achievable.

$$n_s = \frac{\omega\sqrt{V}}{(H_{ad}\,g)^{3/4}} \quad \textit{specific speed}$$

$$d_s = \frac{D(H_{ad}\,g)^{1/4}}{\sqrt{V}} \quad \textit{specific diameter}$$

ω is angular speed (2π*rpm)
V is volumetric flow rate
H_{ad} is the fan pumping head (in meters)
g is the gravitational constant (9.81 m/s^2)

Figure 3 plots the maximum efficiency as a function of specific speed for various compressor types. The figure indicates that for the specific speed of the proposed blower (indicated with red arrows), a "mixed flow" (mixed axial/radial) is an appropriate choice. Figure 4 is a topographical n_s-d_s plot, which shows that the maximum achievable aerodynamic efficiency for the proposed blower should be ~ 80%. Thus the n_s-d_s comparison indicates that the high aerodynamic efficiency required for the proposed blower is feasible.

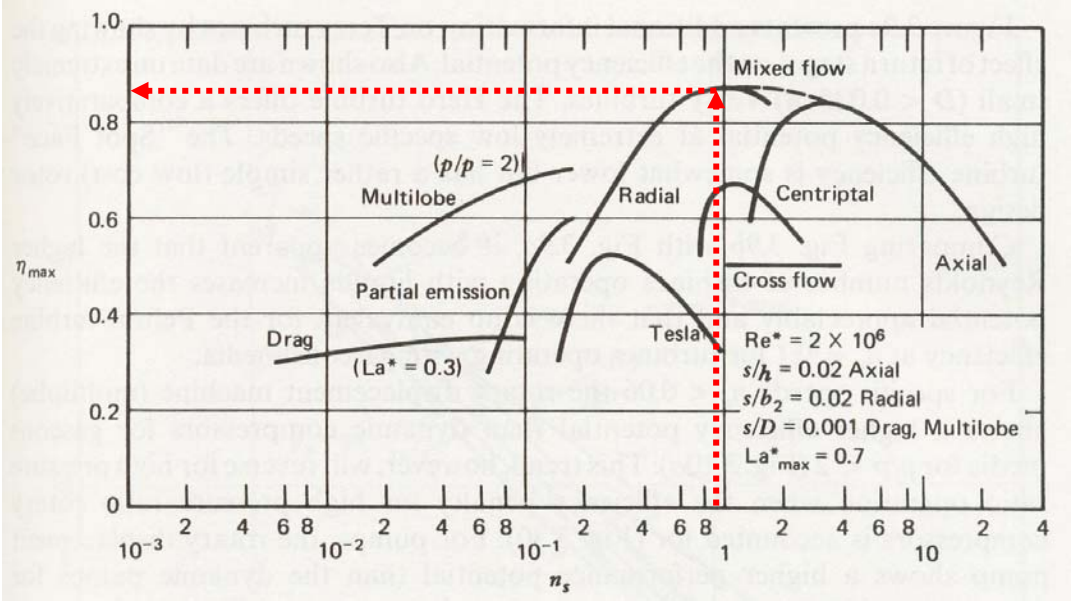

Figure 3: Maximum compressor efficiencies as a function of specific speed (various types) [1].

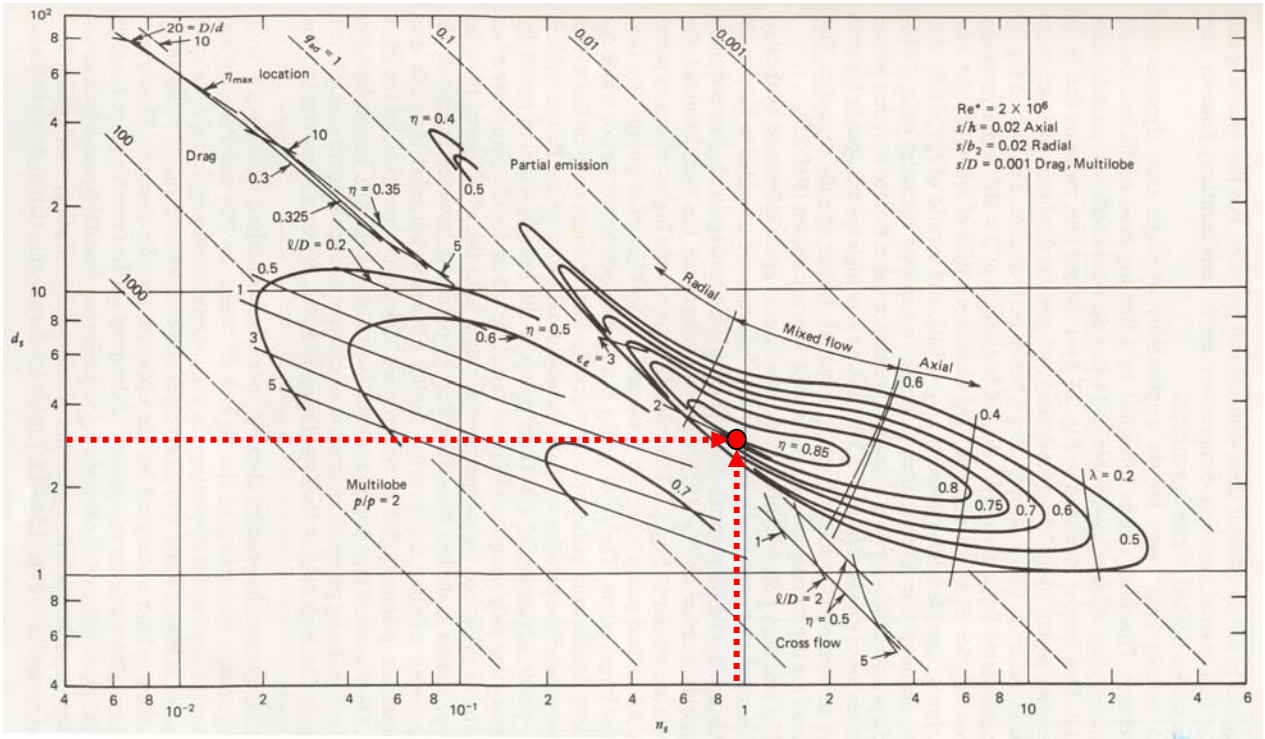

Figure 4: $n_s d_s$ diagram for single stage compressors [1].

3. BLOWER DESIGN

The design of the blower began with establishing a set of geometric variables used to construct the blower. These variables are sub-divided into independent and dependent categories. A known set of independent variables fully constrains the geometric design of the blower. In order to estimate the values of the initial set of independent variables, aerodynamic similarity of turbo-machinery was used.

Aerodynamic Similarity

The proposed blower is aerodynamically similar to an existing centrifugal compressor pictured in Figure 5. The performance plot of this compressor demonstrates a high aerodynamic efficiency. Aerodynamic similarity of turbo-machinery is measured by comparing 3 main attributes:

1) Loading Function (ψ) – ratio of total enthalpy rise (specific work transfer) to KE of blade
2) Flow function (ϕ) – flow handling capability of turbo-machine (choked flow)
3) Geometry – blade height, ID, OD, ratios

The loading function and flow function are defined below. The 3 aerodynamic similarity attribute values are highlighted

Table 1, demonstrating that the two turbo-machines are similar.

$$\Psi = \frac{\Delta h_0}{U^2} \qquad \phi = \frac{\dot{m}\sqrt{RT_0}}{P_0 d^2 \sqrt{\gamma}}$$

Δh_0 = change in stagnation enthalpy
U = blade tip speed
$\dot{m}$ = mass flow rate
γ, R = gas constant and specific heat ratio for air
P_0 T_0 = stagnation temperature and pressure at inlet
d = blade tip diameter at impeller exit

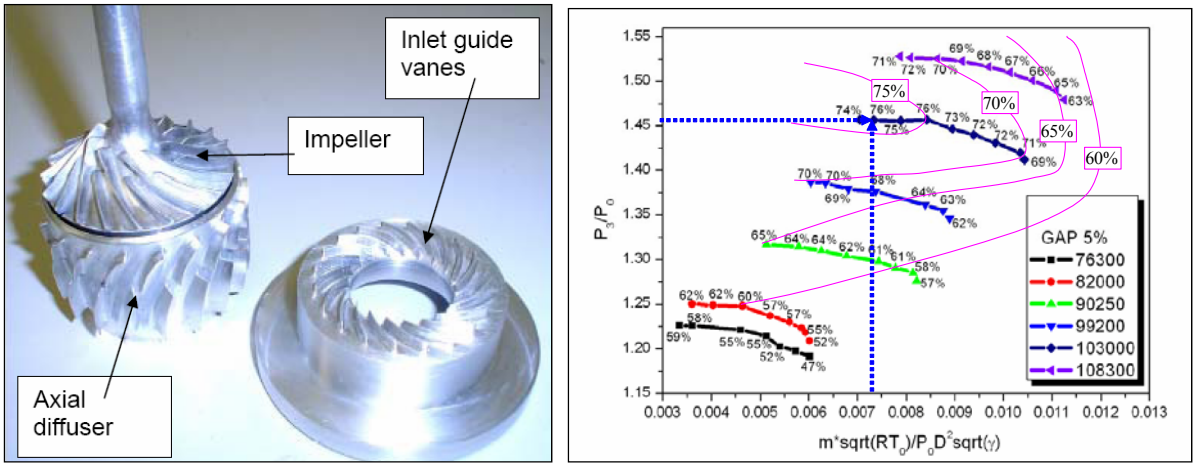

Figure 5: Photo & Performance plot of existing centrifugal compressor

Table 1: Comparison of existing CC and proposed blower

Attribute	Existing CC	Proposed Blower
Diameter (cm)	4.8	4.4
Blade Height (mm)	2	3.4
Speed	103,000	25,000
# blades	20	10
Pressure Ratio	1.46	1.012
Pressure Rise (Pa)	46,000	1243
Mass Flow Rate (g/s)	6.8	5.4
Exit Flowrate (m^3/min, [CFM])	0.36, [13]	0.28, [10]
Isentropic Flow Work (W)	278	6.2
Flow function	0.0073	0.0069
Isentropic Efficiency	73%	55%
Loading function	0.72	0.63
Motor Efficiency	92%	80%
Input Power (W)	360	14

Geometric Parameters

Starting with values established from aerodynamic similarity, a set of independent variables was established for the blower as shown in Table 2. Also listed in the table are the final values of the blower geometry after the Computational Fluid Dynamics (CFD) analysis and design adjustments. Many of the variables are unchanged, indicating that the aerodynamic similarity gave a reasonable starting point for the blower design.

Table 2: Independent variables (dimensions in mm, angles in degrees from axial)

Symbol	Description	Initial Estimate	Final Value
r_i	Impeller inlet hub radius	5	8
α_i	Impeller inlet hub angle	0	0
b_i	Impeller inlet blade height (radial)	4	4
l_b	Impeller length (axial)	10	10
α_e	Impeller exit hub angle	50	50
b_e	Impeller exit blade height (normal)	2.5	3
N_b	# blades	12	12
t_b	Blade & vane thickness	0.5	0.5
t_r	Inlet radial tip gap	0.08	0.08
t_n	Exit normal tip gap	0.05	0.05
N_R	Rotational speed (rpm)	25,000	35,000
c_w	Radial gap b/n rotor & stator hubs	1	1
$r_{d,out}$	Diffuser outside radius	25	25

Symbol	Description	Initial Estimate	Final Value
b_v	Vane height	2	2
l_{ds}	Straight diffuser length	20	20
N_v	# vanes	24	24
N_s	# Diffuser vane segments	3	3
β_2	Relative flow angle at blade exit	20	25
α_{slip}	Blade exit to vane inlet slip angle (relative)	0	6.3
$\dot{V}$	Inlet Volumetric flowrate (CFM)	10	10
ΔP	Blower Pressure Rise (Pa)	1250	1250
T_1	Inlet temperature	35°C	35°C
P_3	Blower Outlet pressure	1 atm	1 atm

A few of the important dependent variables are shown in Table 3 along with their defining equations.

Table 3: Dependent variables

Symbol	Description	Equation
l_g	Blade/vane gap length (steamwise)	$3*b_e$
r_e	Impeller exit hub radius	$r_e = r_i + \frac{l_b}{2}\left[\tan(\alpha_i) + \tan(\alpha_e)\right]$
$r_{i,t}$	Impeller inlet tip radius	$r_{i,t} = r_i + \frac{b_i}{\cos(\alpha_i)}$
$r_{i,s}$	Shroud inlet radius	$r_{i,s} = r_{i,t} + t_r$
$r_{e,t}$	Impeller exit tip radius	$r_{e,t} = r_e + b_e\cos(\alpha_e)$
$r_{e,s}$	Shroud exit radius	$r_{e,s} = r_e + (b_e + t_n)\cos(\alpha_e)$
$l_{b,t}$	Tip-to-tip impeller length	$l_{b,t} = l_b - b_e\sin(\alpha_e)$
$l_{s,t}$	Shroud length (axial)	$l_{s,t} = l_b - (b_e + t_n)\sin(\alpha_e)$
l_{dhi}	Axial location of diffuser hub inlet	$l_{dhi} = l_b + \frac{c_w}{\tan(\alpha_e)}$
r_{dis}	Vane inlet shroud radius	$r_{dis} = r_{e,s} + l_g\sin(\alpha_e)$
l_{dti}	Vane tip inlet shroud axial location	$l_{dti} = l_{s,t} + l_g\cos(\alpha_e)$
r_{dhi}	Diffuser hub inlet radius	$r_{dhi} = r_e + c_w$
r_{dh2}	Vane hub inlet radius	$r_{dh2} = r_{dis} - (r_{e,s} - r_e)$
l_{dh2}	Vane hub inlet axial location	$l_{dh2} = l_{dti} + (b_e + t_n)\sin(\alpha_e)$
$r_{d,in}$	Diffuser inside hub radius inlet	$r_{d,in} = r_{d,out} - b_v$
l_{dm}	Axial length of mixed diffuser	$l_{dm} = \frac{r_{din} - r_{dh2}}{1 - \cos(\alpha_e)}\sin(\alpha_e)$

Symbol	Description	Equation
R_{dm}	Radius of mixed diffuser arc	$R_{dm} = \frac{l_{dm}}{\sin(\alpha_e)}$
P_1	Blower Inlet Pressure	$P_1 = P_3 - \Delta P$

4. CFD ANALYSIS

Having established a geometric design based on an analytical analysis and aerodynamic similarity, the next step is to estimate the blower performance using a Computational Fluid Dynamics (CFD) program. The CFD results enabled adjustment of geometric constraints to mitigate losses and improve efficiency.

Surfaces & Meshing

Since the blower has 12 blades on the impeller, a periodic section is a 30° angular section. However, the 30° section must "twist" to follow the lines of symmetry between blades and/or cut through the middle of the blades and vanes. The periodic section is comprised of 1 blade passage and 2 vane passages. Figure 6 shows a wireframe of the model alongside a single periodic section.

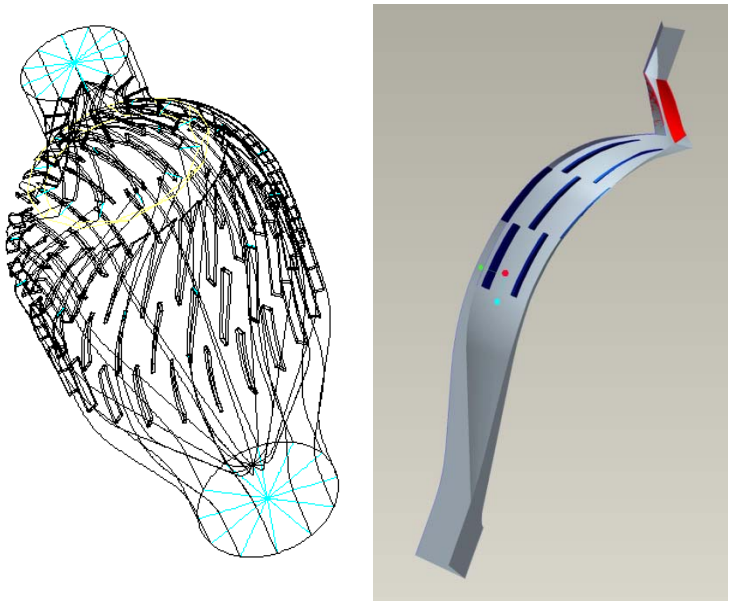

Figure 6: Wireframe model of 12 segments (left), and a single periodic section (right)

For the CFD analysis, only the flow surfaces are important, so most of the solid material can be cut away. Additionally, a surface must be added for the analysis, at the sliding mesh interface between the rotating impeller and the stationary diffuser. Various surfaces of the CFD analysis are shown in Figure 7.

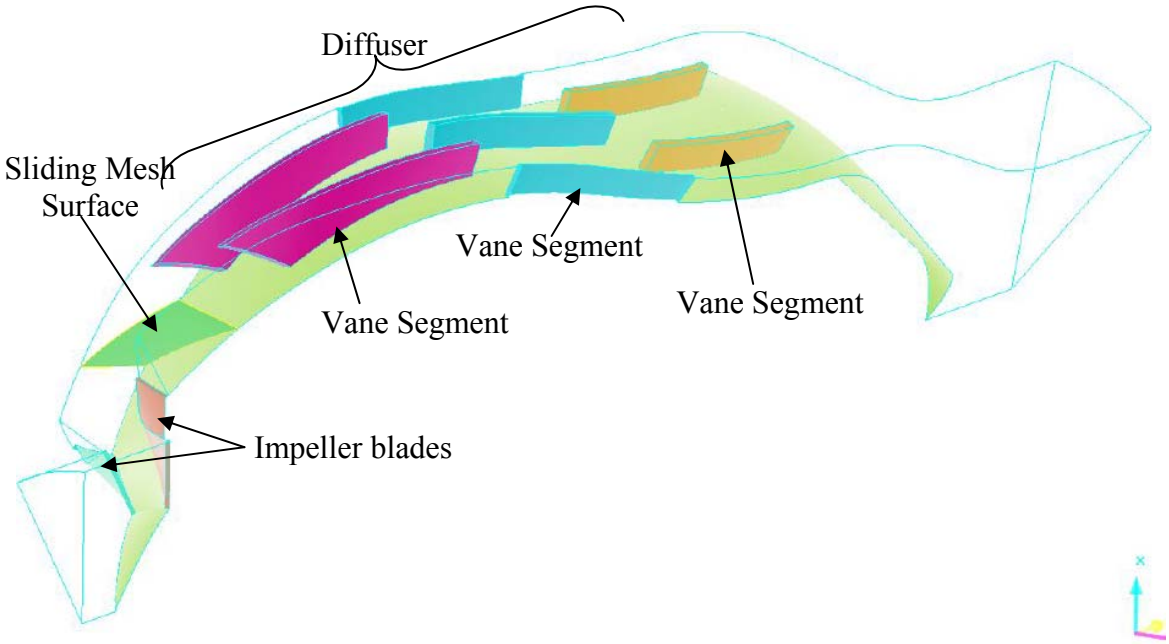

Figure 7: CFD defined surfaces

The resolution of the CFD surface mesh needs to be fine enough to ensure accuracy, yet coarse enough to run a simulation in a reasonable amount of time. A photo of the initial mesh is shown in Figure 8.

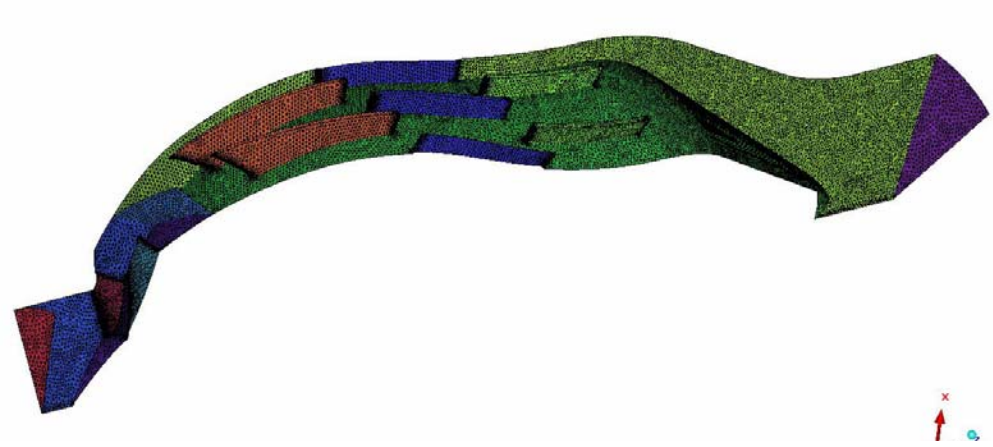

Figure 8: Initial Grid (794593 Cells, 1627326 Faces, 158664 Nodes)

Simulation Details

The analysis involves the examination of the unsteady effects due to flow interaction between the stationary components and the rotating blades. In this study, the sliding mesh capability of FLUENT is used to analyze the unsteady flow in the blower. The rotor-stator interaction is modeled by allowing the mesh associated with the rotor blade row to rotate relative to the stationary mesh associated with the stator blade row.

Various boundary conditions are placed on appropriate surfaces as shown in Figure 9. These include specifying the mass flow rates, outlet pressure, and impeller rpm as well as defining periodic and "walled" surfaces. Walled surfaces are considered to be insulated with a "no-slip" condition.

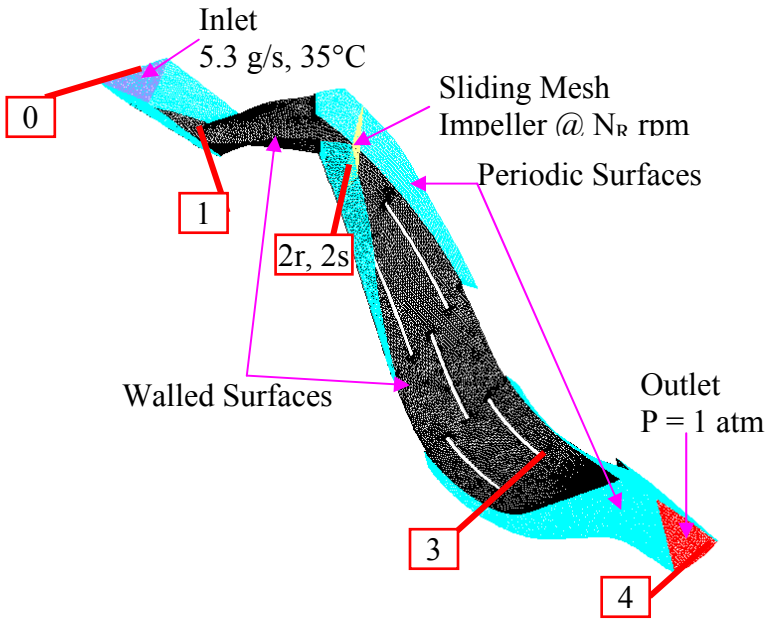

Figure 9: Boundary Conditions of Analysis

Some information specific to the FLUENT software for the simulation includes the following:

a. Density Based Solver
b. Implicit Formulation
c. Unsteady
d. 2nd-Order Implicit Unsteady Formulation
e. Turbulence model: Renormalized k-ε
f. Near wall treatment: wall functions

The periodic time step is the time it takes for consecutive blades of the impeller to pass a fixed node on the diffuser. This time step is a function of the rpm and # blades of the impeller:

$$\tau_{period} = \frac{60}{N_R \cdot N_b}$$

At 25,000 rpm with 12 blades, this time step is 0.2 ms. In the CFD analysis, the initial time step is an integer factor smaller than this number (i.e. 1/4). As periodic waveforms begin to appear in the pressure and velocity history plots, the time step is reduced to 1/20th this number for final convergence of the model. Convergence is checked by comparing 2 consecutive 100 step calculations for similarity.

The CFD analysis generates a solution by solving the flow, turbulence and energy equations. The air is assumed to be an ideal gas, and the SIMPLE algorithm (Semi-Implicit Method for Pressure-Linked Equations) is used for pressure-velocity coupling. Second order up-wind is used for density, momentum, turbulent dissipation rate, turbulent kinetic energy and energy. For pressure, the standard discretization scheme is used.

5. CFD RESULTS

The 1st CFD run was completed twice with 2 meshes: the 2nd being finer than the 1st. Agreement between the two meshes suggested that the mesh resolution was sufficient for accurate results. Results of the CFD analysis are analyzed by creating the following:

1) Tabulated Velocity, Static Temperature and Pressure (P_s, T_s) vs. position @ points "0" (circular entrance), "1" (impeller entrance), "2r" (sliding vane mesh, rotor side), "2s" (sliding vane mesh diffuser {stator} side) "3" (diffuser exit), and "4" (circular exit)
2) History plots of velocity and temperature vs. time step
3) Contour and streamline plots of pressure and velocity

Due to the low pressure ratio of the blower, the pressures converge faster than the total enthalpy used to calculate the required shaft power. Thus, when it became apparent in the 1st CFD run at 25,000 rpm that the pressure rise was insufficient; the speed was increased to 35,000 – the max speed of the desired motor. This was the 2nd CFD run. This run was allowed to get closer to convergence on total enthalpy to give an initial shaft power estimate for the blower.

Each successive CFD run uses the same conditions. The differences between runs lie in the specific geometry such as blade/vane angles and positions. The major parameters that set these values are summarized in Table 4. The table also contains 3 important CFD output results: gross total pressure rise, net static pressure rise, and shaft power.

Table 4: CFD Parameters and Results for Each Run

	1st Run	2nd Run	3rd Run	4th Run	5th Run	6th Run	Target
Impeller rpm	25,000	35,000	35,000	35,000	35,000	35,000	-
r_i (mm)	5.0	5.0	8.0	8.0	8.0	8.0	-
β_2 (deg)	20	20	25	25	25	25	-
b_e (mm)	2.5	2.5	3.0	3.0	3.0	3.0	-
α_{slip} (deg)	0.0	0.0	0.0	7.1	6.0	6.3	-
Gross Total ΔP (Pa)	495	1199	1884	1896	2011	2013	-
Net Static ΔP (Pa)	170	660	240	1108	1243	1253	1243
Shaft Power (W)	n/a	7.6	10.8	9.9	10.2	10.2	11

The gross total pressure rise is the change in total pressure of the air after the work done by the impeller. In a 100% efficient blower decelerating the flow all the way to zero velocity, this is the maximum possible static pressure that can be generated. So obviously, this number should be significantly higher than the 1243 Pa required static pressure rise. The 3rd CFD run was the first run where the total pressure rise was sufficiently high, but the losses were also high, and the net static pressure rise was only 240 Pa. Thus, in the 4th run, α_{slip} (defined as the relative angle between the impeller blade exit and diffuser vane inlet) was adjusted to reduce losses. Runs 5 and 6 further adjusted the flow angle to an optimal value.

Detailed tabulated results of Run 6 are shown Table 5 at various plane locations of the blower. The total pressure losses (ΔPt) within the diffuser are a measurement of flow separation and isentropic inefficiency. The required shaft power can be calculated from the change in total

enthalpy (Δht) multiplied by the mass flow rate (5.3 g/s). Because only the impeller does work on the fluid, the only change in total enthalpy should be from 1 to 2r. The non-zero numbers in the table reflect the accuracy limits of the analysis, but it is important to note that they are less than 2% of the total enthalpy change.

Table 5: Tabulated CFD Results (6th Run)

	Plane	ht	Δht	hs	Δhs	Pt	ΔPt	Ps	ΔPs	Total temp	ΔTt	Static temp	ΔTs	Velocity magnitude	Axial Velocity
		j/kg	j/kg	j/kg	j/kg	Pa	Pa	Pa	Pa	K	K	K	K	m/s	m/s
0	circular inlet (0)	9914.5		9861.1		100173.3		100113		308		307.95		11.18	10.009
1	impeller inlet (1)	9917.96	**3**	9640.5	**-221**	100168.4	**-5**	99853.9	**-259**	308	**0**	307.73	**-0.22**	22.495	21.096
2	sliding interface rotor (2r)	11800.5	**1883**	11067.4	**1427**	102181.5	**2013**	101237.6	**1384**	309.9	**1.9**	309.15	**1.42**	39.346	9.24
3	sliding interface stator (2s)	11800.3	**0**	11067	**0**	102179.5	**-2**	101238.5	**1**	309.9	**0**	309.15	**0**	39.65	9.004
4	diffuser vane 1 exit (v1)	11784.9	**-15**	11166.2	**99**	101759.3	**-420**	101053.2	**-185**	309.9	**0**	309.25	**0.1**	34.672	18.363
5	diffuser vane 3 exit (3)	11811.1	**26**	11620.3	**454**	101476.7	**-283**	101259.1	**206**	309.9	**0**	309.7	**0.45**	18.892	18.284
6	circular exit (4)	11825.1	**14**	11768.2	**148**	101427.6	**-49**	101366.1	**107**	309.9	**0**	309.83	**0.13**	10.54	8.256
	Exit - Inlet		**1911**		**1907**		**1254**		**1253**		**1.9**		**1.88**		

Convergence of each CFD run can be verified by examining the time history plots of velocity and temperature as shown in Figure 10. Note that the temperature only begins to converge after the velocity has reached near-convergence.

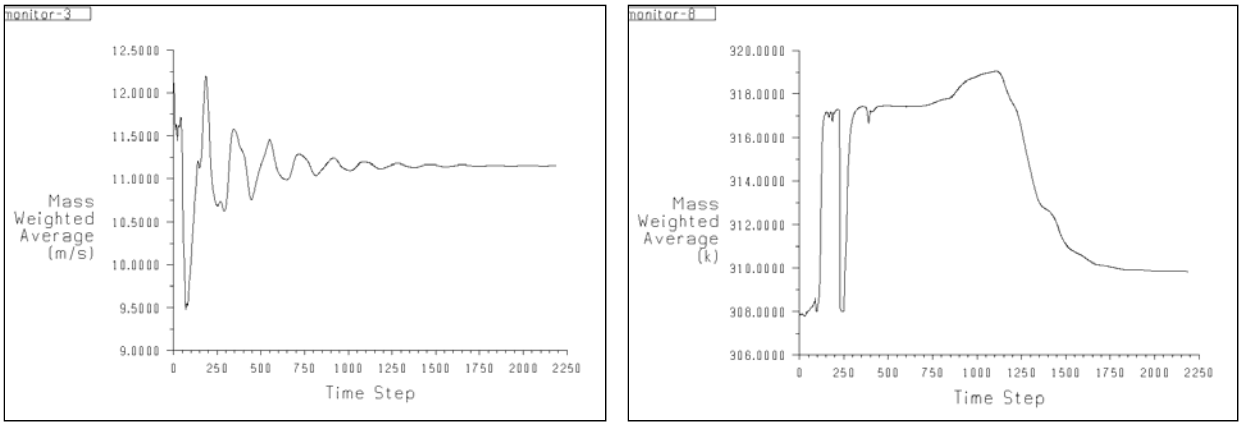

Figure 10: Convergence Plot of Velocity (left) and Temperature (right)

Flow angle correction

An important parameter adjusted in subsequent CFD run is α_{slip}, defined as the relative angle between the impeller blade exit and diffuser vane inlet. The adjustments made to α_{slip} are estimated by examining the velocity vector field and pressure plot outputs of the analysis. The adjustment is proportional to the angle measured between the vane and the velocity vectors when viewing normal to the flow surface. The effect of increasing α_{slip} is to "turn" the vane into the flow. When α_{slip} is under-corrected, a high pressure stagnation region forms "below" the vane, and a low-pressure separation region occurs "above" the vane. When α_{slip} is over-corrected, the high and low pressure regions flip-flop to opposite sides of the vane. This is shown pictorially in Figure 11. Figure 12 and Figure 13 show the pressure plots of Run 3 and Run 4, respectively. Note that Run 3 has an under-corrected α_{slip}, while Run 4 is slightly over-corrected. Figure 14 shows how the correction angle is measured in Run 3 to estimate a new value for α_{slip}.

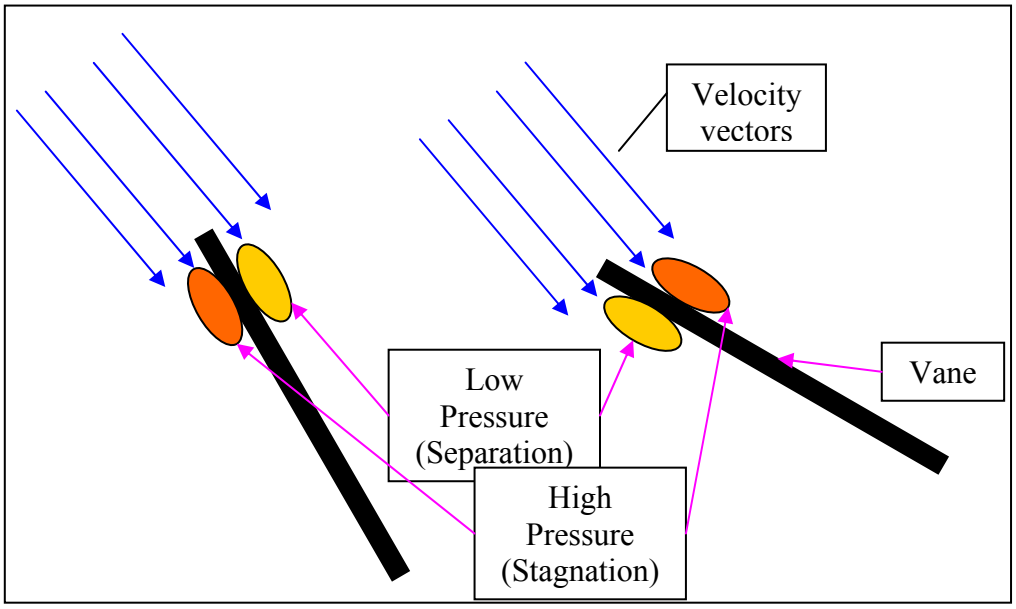

Figure 11: Flow and pressure with α_{slip} a) under-corrected [left] b) over-corrected [right]

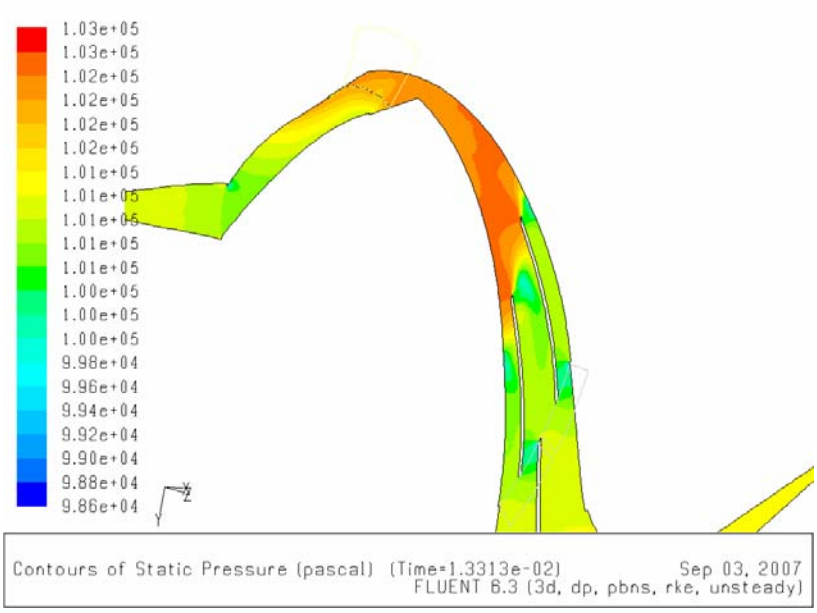

Figure 12: Pressure Plot under-corrected α_{slip} (Run #3)

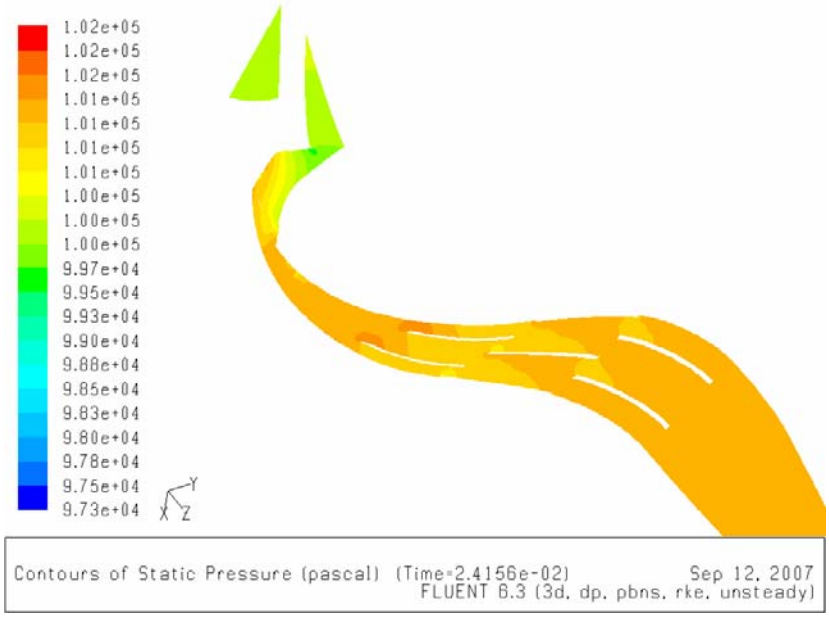

Figure 13: Pressure Plot, over-corrected α_{slip} (Run#4)

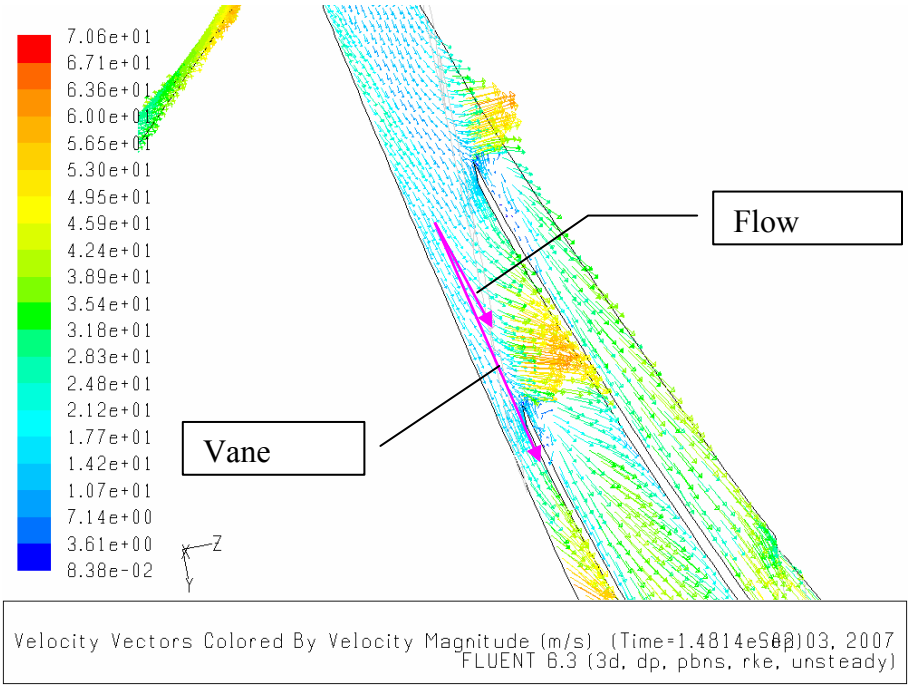

Figure 14: Flow Separation and α_{slip} correction measurement (Run #3)

Further Blower Improvements

With adjustment and refinement of the blower flow angles, the feasibility of the blower design has been established. While there is still room for tweaking of the diffuser design (# vane segments, individual vane angles, etc.), the next logical step in the blower development is to build and test a prototype blower. Test results will then be compared to CFD outputs to ensure agreement, and may lead to adjustments in the CFD model. Once the CFD and prototype yield consistent results, then final parameter tweaking on the CFD model can be accomplished, resulting in a 2nd improved prototype to be built and tested.

6. MOTOR AND BATTERIES

The Phase I design shaft power requirement is 10.2 W at 35,000 rpm. A brushless DC motor from Maxon Motors (# 201162) has been identified as a good candidate for the blower. It is 22 mm in diameter and 50 mm long, features integrated electronics, and weighs only 85 g. A technical drawing of the motor is shown in Figure 15. This motor is able to meet the power requirements at 24 V and 76% efficiency as shown in Figure 16. The blower has been designed such that the impeller will mount directly onto the shaft of this motor with no additional bearings required. Thus, the electrical power required is 10.2 / 0.76 = 13.5 W. With the known voltage power, and run time, a suitable battery can be identified.

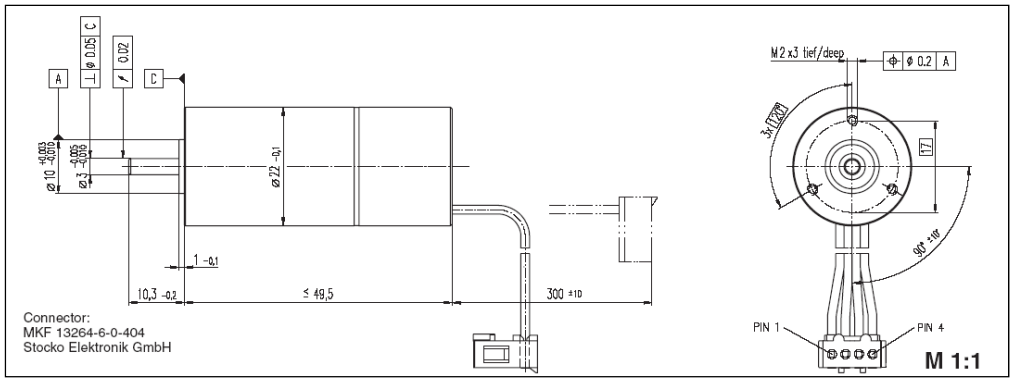

Figure 15: Maxon 201162 Technical Drawing

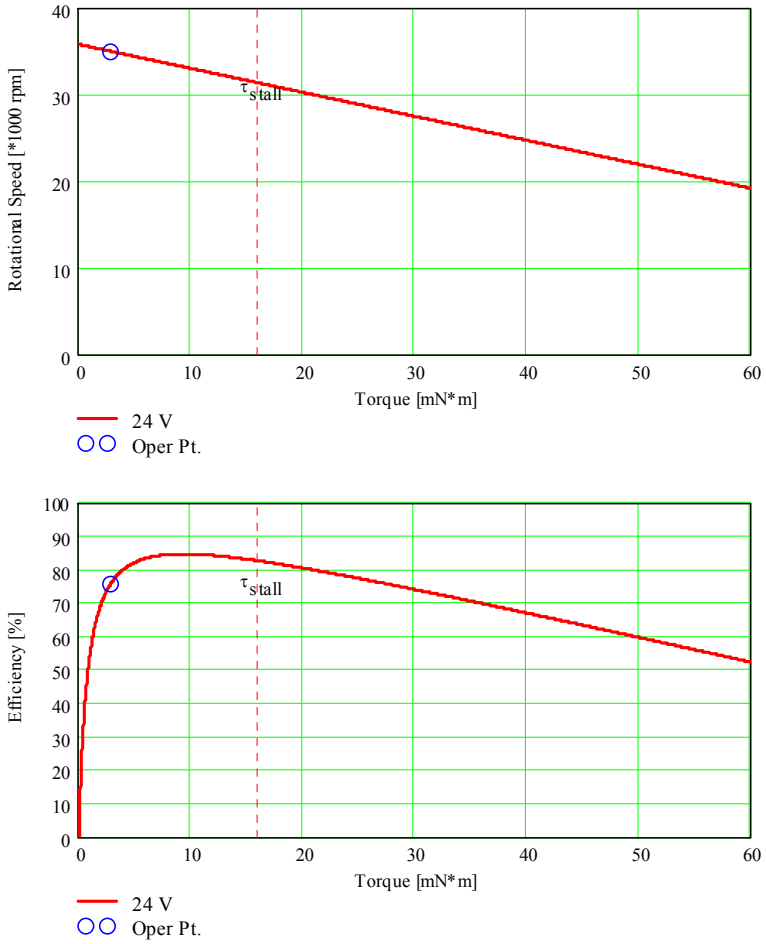

Figure 16: Motor Performance at 24 V with operating point indicated

Table 6 lists a wide range of suitable battery cell combinations based on 4 chemistries available from Saft®: Li-MnO_2, Li-SiO_2, Li-$SOCl_2$, and rechargeable Li-ion. This battery analysis uses just the cells available from one manufacturer, but is representative of what is available in the market. The table lists only those combinations that can meet the 24 voltage requirement and run for at least 4 hours. The "best" cell combination for each battery chemistry is highlighted in Table 6. The Li-$SOCl_2$ has by far the highest energy density, and would last over 10 hours, but

is also the most toxic. The Li-ion combination lasts over 5 hours and has the advantage of being rechargeable, but with the penalty of increased weight. Moving forward in the current size & weight analysis, a representative battery will be assumed to weigh 400 g and have the form factor of 9 "C" sized cells.

Table 6: Suitable Saft® battery cell combinations

Chemistry	Cell Type	Cell Size	Nominal Voltage (V)	Nominal Drain (mA)	Max Current (A)	Nominal Capacity (Ah)	Nominal Energy (W-hr)	Cell Weight (g)	Energy Density (W-hr/kg)	Battery Configuration	Nominal Battery Voltage	Battery Current	Drain /cell	Run Time (hr)	Total Weight (gram)
Li-MnO_2	LM 17130	1/3 A	2.7	4.5	0.3	0.5	1.35	8	169	9 S 5 P	24.3	0.56	0.11	4.5	360
Li-MnO_2	LM 22150	1/3 sub-C	2.7	40	0.4	0.9	2.43	15	162	9 S 3 P	24.3	0.56	0.19	4.9	405
Li-MnO_2	LM 26500	C	2.7	200	1.5	4.5	12.15	60	203	9 S 1 P	24.3	0.56	0.56	8.1	540
Li-SO_2	G 04/3	1/2 AA	2.8	50	0.25	0.45	1.26	8	157.5	9 S 5 P	25.2	0.54	0.11	4.2	360
Li-SO_2	G 06/2	AA	2.8	80	0.5	0.95	2.66	15	177	9 S 3 P	25.2	0.54	0.18	5.3	405
Li-SO_2	G 32/3	2/3 A	2.8	80	0.75	0.8	2.24	12	187	9 S 3 P	25.2	0.54	0.18	4.5	324
Li-SO_2	G 36/2	"long" A	2.8	80	1.5	1.7	4.76	18	264	9 S 2 P	25.2	0.54	0.27	6.3	324
Li-SO_2	LO 34 SX	1/3 C	2.8	80	1.0	0.86	2.408	18	134	9 S 3 P	25.2	0.54	0.18	4.8	486
Li-SO_2	G 52/3	C	2.8	1000	2.5	3.2	8.96	47	191	9 S 1 P	25.2	0.54	0.54	6.0	423
Li-SO_2	LO 29 SHX	C	2.8	250	2.5	3.75	10.5	40	263	9 S 1 P	25.2	0.54	0.54	7.0	360
Li-SO_2	G 54/3	5/4 C	2.8	200	2.5	5	14	58	241	9 S 1 P	25.2	0.54	0.54	9.3	522
Li-SO_2	LO 43 SHX	5/4 C	2.8	200	2.5	5	14	53	264	9 S 1 P	25.2	0.54	0.54	9.3	477
Li-SO_2	LO 40 SX	2/3 "Thin" D	2.8	120	2	3.5	9.8	40	245	9 S 1 P	25.2	0.54	0.54	6.5	360
Li-$SOCl_2$	LS 26180	1/3 C	3.6	10	0.4	1.2	4.32	24	180	7 S 2 P	25.2	0.54	0.27	4.5	336
Li-$SOCl_2$	LSH 14	C	3.6	15	1.3	5.5	19.8	51	388	7 S 1 P	25.2	0.54	0.54	10.3	357
Li-ion (rechargeable)	MP 144350	14.5x43x50mm	3.75	500	2.6	2.6	9.75	68	143	7 S 1 P	26.25	0.51	0.51	5.1	476

7. BLOWER SYSTEM MODEL

A 3D model of the complete blower design has been made, including the battery cells. Figure 17 shows pictures and cross-sections of the model. A weight and volume estimate of the blower is shown in Table 7. The volume is the envelope of space occupied by the blower, such that a 2" diameter is assumed to occupy a 2" x 2" square. Since the motor is contained inside the blower, it does not contribute to the volume.

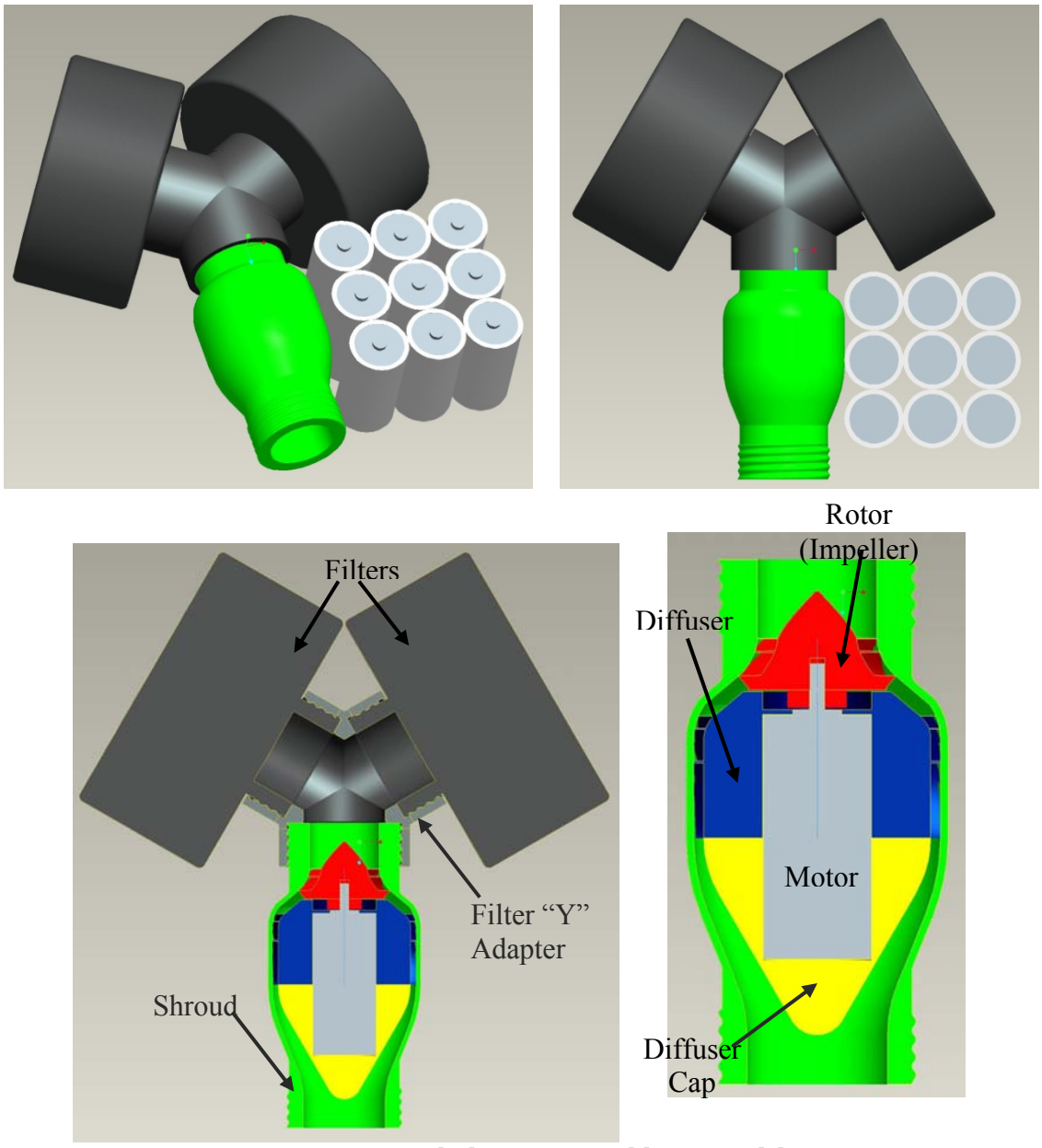

Figure 17: Final Phase I Design blower model

Table 7: Blower Weight and Volume Estimate

	Material	Weight		Envelope Volume
		g	lb	(in^3)
Blower	Aluminum	268	0.59	19
Motor	Actual	85	0.19	-
Filter Adapter	Nylon	42	0.09	9
Battery	Cells	400	0.88	18
TOTAL	-	795	1.75	46

8. CONCLUSIONS

This Phase 1 effort has successfully established the feasibility of the PAVS blower. Table 8 shows that the Phase I design meets or exceeds all of the weight, volume, and performance requirements. A stereo-lithograph model of the blower was built and delivered, demonstrating basic functionality. At this point, a prototype blower has been designed and is ready to be built and tested as part of a Phase II effort.

Table 8: Phase I Design vs. Requirements

Parameter	Requirement	Phase I Design
Air Flow (CFM)	10	10
Pressure Rise (Pa)	1243	1253
Electrical Power (W)	15	13.5
Run Time (hr)	4	5 to 10 (depends on battery chemistry)
Weight (lb)	2	1.8
Volume (in^3)	60	46
Depth (in)	2	2

9. REFERENCES

[1]. Balje, O. E., Turbomachines: A Guide to Design, Selection, and Theory. John Wiley & Sons, 1981. (ISBN 0-471-06036-4)

This document reports research undertaken at the U.S. Army Natick Soldier Research, Development and Engineering Center, Natick, MA, and has been assigned No. NATICK/TR- 15/012 in a series of reports approved for publication.